Phenomenological theory of the dynamics of polymer melts. I. Analytic treatment of self-diffusion

Jeffrey Skolnick,[a] Robert Yaris, and Andrzej Kolinski[b]
Institute of Macromolecular Chemistry, Department of Chemistry, Washington University, St. Louis, Missouri 63130

(Received 16 July 1987; accepted 5 October 1987)

In the context of dynamic Monte Carlo (MC) simulations on dense collections of polymer chains confined to a cubic lattice, the nature of the dynamic entanglements giving rise to the degree of polymerization n, dependence of the self-diffusion constant $D\sim n^{-2}$ is examined. Consistent with our previous simulation results, which failed to find evidence for reptation as the dominant mechanism of polymer melt motion [J. Chem. Phys. **86**, 1567, 7164, 7174 (1987)], long-lived dynamic entanglement contacts between pairs of segments belonging to different chains are extremely rare and are mobile with respect to the laboratory fixed frame. It is suggested that dynamic entanglements involve the dragging of one chain by another through the melt for times on the order of the terminal relaxation time of the end-to-end vector. Employing the physical description provided by the MC simulation, the general expression of Hess [Macromolecules **19**, 1395 (1986)] for the friction constant increment experienced by a polymer due to the other polymers forms the basis of a phenomenological derivation of $D\sim n^{-2}$ for monodisperse melts that does not require the existence of reptation. Rather, such behavior is dependent on the relatively benign assumptions that the long distance global motions of the chains are uncorrelated, that the dynamic contacts can be truncated at the pair level, and that the propagator describing the evolution between dynamic contacts contains a free Rouse chain component. The mean distance between dynamic entanglements is predicted to depend inversely on concentration, in agreement with experiment. Moreover, as the free Rouse component is frozen out, for chains greater than an entanglement length n_e, a molecular weight independent glass transition is predicted. Extension to bidisperse melts predicts that the probe diffusion coefficient D_p depends on the matrix degree of polymerization, n_m, as n_m^{-1}. Finally, comparison is made between the theoretical expressions and MC results for mono- and bidisperse melts.

I. INTRODUCTION

The development of a model adequate to describe the diffusive and viscoelastic properties of concentrated solutions and melts of long chain polymer molecules has been a problem of long standing.[1-4] The most striking experimental results which must be explained by a successful model are the way that the diffusion constant and viscosity of dense polymeric systems scale with the molecular weight (or degree of polymerization, n). The center-of-mass self-diffusion constant D scales like

$$D\sim n^{-1}, \quad n<n_c', \tag{1.1a}$$

$$D\sim n^{-2}, \quad n>n_c', \tag{1.1b}$$

where n_c' is a critical degree of polymerization (although recently other $D\sim n^{-\alpha}$ have been reported[5,6]). The scaling behavior of the zero frequency shear viscosity η is

$$\eta\sim n^{1}, \quad n<n_c, \tag{1.2a}$$

$$\eta\sim n^{3.4}, \quad n>n_c. \tag{1.2b}$$

Observe that the crossover regions for viscosity and diffusion are not the same with

$$n_c<n_c'. \tag{1.3}$$

A key experimental observation towards the understanding of the behavior of polymer melts is the response of a melt to a sudden deformation (shear). At very short times, the melt behaves elastically like a rubber which is a crosslinked collection of chains. At later times, the polymer melt relaxes and behaves like a viscous fluid. This suggests that the entanglements of the chains in the polymer melt behave at short times much the same as the crosslinks in a rubber. However, unlike the rubber where the crosslinks between chains are chemical bonds and hence "infinitely" long lived, the chains in the melt eventually slide past the physical entanglements. The importance of chain entanglements has been emphasized by Edwards.[7] This resulted in the reptation model of deGennes,[2,3,8] and Doi and Edwards.[9] An alternative kinetic theory approach of Curtiss and Bird[10] based on anisotropic bead friction tensors should also be mentioned at this point.

In the reptation model, the motions of a chain are constrained to a tube composed of the entanglement points formed from the other chains in the melt. Hence the dominant motion of a chain is a slithering motion down the tube (whence the name reptation) past entanglement points. It is assumed (at least in the original reptation model) that the entanglements remain static for a time on the order of a re-

[a] Alfred P. Sloan Foundation Fellow.
[b] Permanent address: Department of Chemistry, University of Warsaw, 02-093, Warsaw, Poland.

 0021-9606/88/021407-11$02.10

laxation time of the polymer end-to-end vector—thus reducing the many-body problem to a one-body problem. This assumption that the chain mostly moves along its original contour, with lateral motion being unimportant, allows for the solution of the problem. Due to the convoluted path (when viewed from the laboratory fixed frame) down which the chain must diffuse, the diffusion constant scales as n^{-2}. Similarly, the terminal relaxation time of the end-to-end vector, τ_{rep} (frequently referred to as the tube disengagement time), scales as n^3. Combining τ_{rep} with the assumption of rubber-like behavior at short times gives $\eta \sim \tau_{rep} \sim n^3$. Thus this simple model almost reproduces the experimental scaling behavior of diffusion and viscosity—one should note, however, that it does not explain the different crossover regimes for D and η, Eq. (1.3).

The reptation model, with modifications to treat all of the chains self-consistently,[11,12] has been the accepted model of polymer melt dynamics for the past 15 years. Most recently, Hess[13] attempted a microscopic derivation of reptation using a many-body approach. He assumed that the interchain, repulsive excluded volume interactions result in forces perpendicular to the chain contour and thereby lead to chain motion along the chain contour, i.e., reptation (of course this conclusion was inescapable given the assumed interaction). The one small fly in the ointment was that none of the computer simulations which treated all chains equivalently obtained the detailed reptation model predictions.[14] However, all the simulations were for relatively short chains and were not at high concentrations and hence tended to be discounted as irrelevant.

With this in mind we recently completed a series[15–18] of dynamic Monte Carlo (MC) lattice simulations of dense systems of chains up to $n = 800$, which by all the standard criteria are entangled. Hence reptation should have been evident if, in fact, it were present. We saw no evidence of reptation as the dominant mechanism of chain motion. In this paper and the companion paper we will construct a new model of the diffusive and viscoelastic behavior of polymer melts incorporating what we have learned from the computer simulations. Since we are treating the simulations as a set of experiments, albeit computational experiments, in Sec. II we shall review the findings from these computer experiments and the conclusions drawn from them. It is here that the key physical assumptions of the model will be made and justified. We shall introduce the idea of a dynamic entanglement and make the important distinction between a dynamic entanglement and a physical contact. In Sec. III, we shall fit these physical assumptions into Hess' many-body theory to obtain a treatment for dense polymer diffusion. It will be shown that the $D \sim n^{-2}$ behavior, which has been widely interpreted as experimental evidence for reptation, is a quite general result obtainable under very weak assumptions and is not tied to the reptation model. This will be followed by a brief discussion. The treatment of the viscoelastic behavior of polymer melts requires a more detailed model and hence is separated from the general treatment of diffusion and appears in the companion paper.[19] In this second paper we will not only obtain the viscoelastic behavior of the melt embodied in Eq. (1.2) but also show why the viscosity crosses over to entangled behavior at a different molecular weight than does the diffusion constant.

II. RESULTS OF COMPUTATIONAL EXPERIMENTS

In order to simulate the behavior of dense collections of long polymer chains for the long times necessary to enable them to exhibit true diffusive behavior [where both the mean-square single bead displacement $g(t) \sim t$ and the mean-square displacement of the center-of-mass, $g_{c.m.}(t) \sim t$] lattice dynamic Monte Carlo simulations were performed. The diffusive regime begins when $g_{c.m.}(t) > 2\langle S^2 \rangle$, where $\langle S^2 \rangle$ is the mean-square radius-of-gyration of a chain. It is not possible, given the present state of computers, to come even close to the diffusion limit for long chain dense systems using molecular dynamics or off-lattice Monte Carlo simulations. Even using lattice MC required months of computing on a dedicated μVAX-II for a single set of runs, with the total set of simulations requiring $\sim 1\frac{1}{2}$ CPU years on one and sometimes two dedicated computers.

The set of simulations on monodisperse homopolymeric chains spanned a range of volume fraction of occupied lattice sites, ϕ, from zero to 0.75 and for chains of length up to $n = 216$ for a diamond lattice[16] and chain lengths ranging from $n = 64$ to $n = 800$ for $\phi = 0.5$ on a cubic lattice.[17] The MC lattice moves were chosen to span the space of allowable moves. Where possible, the properties of the chains were studied and compared with analytic theories and off-lattice simulations to demonstrate that the lattice produced negligible effects on the long time results. Furthermore, if allowance is made for the difference in the local persistence lengths, i.e., a diamond lattice chain of length n is dynamically equivalent to a cubic lattice chain of length $n/2$, identical results are found for the two lattices. Hence we have evidence that the long time dynamics we are interested in are not lattice artifacts (the reader is urged to read our earlier simulation papers[16–18] for further evidence).

It was found that one could obtain a diffusion constant and a terminal relaxation time that scaled properly with the molecular weight, i.e., given by Eqs. (1.1b) and (1.2b). It was also found that there was no regime where $g(t) \sim t^{1/4}$ contrary to the prediction of the reptation model. In this we agreed with all previous simulations[14] on shorter and less dense systems of chains. It should be pointed out that especially for the $\phi = 0.5$, $n = 800$ chains on the cubic lattice, by all criteria we were in the entangled regime and should see evidence of reptation if it exists.

A. Do chains reptate?

In order to definitively answer whether our simulated systems of chains diffuse by reptation we analyzed the motion of the chains by a method similar to the primitive path analysis of Doi and Edwards.[9] They replaced the actual chain by an equivalent chain where all the local fluctuations irrelevant to the diffusive motion are averaged out. We constructed such an equivalent chain by replacing each bead on the original chain by a point on the equivalent chain which is the center-of-mass of a subchain composed of n_B beads. This gives a smooth average path composed of the centers-of-

mass of the overlapping subchains which should be very close to Doi and Edwards primitive path if n_B is approximately equal to the entanglement length.

We construct such an equivalent chain at each time step (and also for each chain in the system). We can then analyze the motion of these equivalent chains. The equivalent chain at some initial time (defined to be zero) defines a spatial curve which can be used to generate a local curvilinear coordinate system. We then project the primitive path at later times back onto the zero time path and obtain the components of the motion parallel and perpendicular to the zero time path. The reptation model demands that for times longer than that required for the diffusion to the walls of the tube but shorter than the tube renewal time (i.e., the terminal relaxation time) the dominant motion of the central portion of each chain must be along the primitive path. What was observed in all cases was that after a short time preference for transverse motion (which is not relevant to the long time motion and has been explained elsewhere[15]), the motion of the equivalent path is essentially isotropic. Therefore, there cannot be a tube confining the chain motions and reptation cannot be the dominant diffusive mechanism.

As a check that we were not somehow or other disallowing reptation by our choice of lattice moves, we also simulated a system where a single mobile chain was surrounded by a matrix of frozen chains.[16] The frozen chain matrix was rigidly pinned every 18 beads but was allowed to move between the pins. Here the separation of time scales necessary for the reptation model is rigorously true and reptation should be observed. When we performed the equivalent path analysis for the mobile chain in the frozen environment we did indeed observe reptation, i.e., the dominant motion was along the primitive path contour (although the chain kept trying to leak out of the tube).

As a further check on the question of time scale separation, we performed a series of simulations[18] for a probe chain of degree of polymerization $n_p = 100$ dissolved in a series of matrix polymers of degree of polymerization $n_m = 50$, 100, 216, and 800, all at a total volume fraction $\phi = 0.5$. In one sense, since the diffusion constants differ by about two orders of magnitude, there is the separation of time scales required by the reptation model between the probe chain and the matrix for the case $n_m = 100$ and $n_p = 800$. However, although there is a global time scale difference between the probe chain and the matrix, there is not a local time scale difference since all chains are free to move in the same way. The diffusion constant of the probe chain decreases by about 25% as the matrix chains increase from $n_m = 50$ to 800 consistent with the experimental results on polystyrene.[20,21] However, when the equivalent path analysis was performed on the motion of the probe chain, the motion once again was isotropic.

In all cases of monodisperse and bidisperse melts, we also examined snapshot pictures of the evolution in time of the equivalent path and significant transverse motion with negligible motion along the primitive path was observed. Hence, we are forced to conclude that in a melt or dense solution when all chains are free to move the interchain entanglements do not constrain the motion of the chain to be along the primitive path. *The chains do not diffuse by reptation.*

B. The nature and importance of dynamic entanglements

In the reptation model the entanglement points serve to define the tube down which each chain diffuses. If this is the case, the mean distance between entanglements n_e must be small compared to the length of the chain. Otherwise if the distance between entanglements is large, the chain will easily leak out of the tube. That is, if n_e is large, loop entropy will not be large enough to constrain the chain. However, the behavior of the chains was similar to that of a Rouse chain,[22,23] albeit a renormalized Rouse chain; hence the nature and effect of entanglements must be reexamined.

The first thing one must realize is that for an entanglement to have an important effect on the long distance diffusive behavior it is not enough for two chains to be in contact—they must remain in contact for a time of the order of a terminal relaxation time. Thus we will distinguish between interchain static entanglements and dynamic entanglements by their time evolution. Static entanglements are mostly interchain contacts where the chains quickly, on the time scale of the terminal relaxation time, diffuse apart (remember that locally the diffusive motion of a chain is predominantly transverse to its chain contour). Thus, most of the chain entanglements are static entanglements. Occasionally two chains are not only entangled and in contact but are also randomly diffusing in the same direction. If they continue to be in contact for a time of the order of the terminal relaxation time, we refer to such an entanglement as a dynamic entanglement. When such a dynamic entanglement occurs, a chain appears to drag another chain through the melt for a period on the order of a terminal relaxation time. Of course eventually these two chains will also diffuse apart; the only difference is that this happens on a much longer time scale. Even the simplest considerations would suggest that dynamic entanglements are much less common than static entanglements and that the mean distance between dynamic entanglements is large compared to the mean distance between shorter lived contacts.

Before examining the differing effects on the diffusive behavior of these two types of entanglements we will examine our computer experiments to verify that the above physically motivated conjectures are consistent with the simulations. We employed the following procedure:

(i) The actual chain was replaced by a series of nonoverlapping blobs each containing n_B monomers, where n_B is the number of monomers down a chain over which the static excluded volume effects are felt (the static excluded volume screening length). This is essentially a pearl necklace model of the polymer.

(ii) We then searched for pairs of blobs (or pearls) where each blob belongs to a different chain and whose centers-of-mass are less than a distance $r_{\min}$ apart at zero time.

(iii) The fraction of such contacts that are still surviving at a time t later, $n_c(t)$ are counted.

(iv) The mean-square displacement of the center-of-mass of the contact pair of blobs was computed with respect to the laboratory frame, $g_{\rm lab}(t)$. The mean-square relative displacement of the two blobs $g_{\rm rel}(t)$ was also computed.

In Fig. 1, we plot $n_c(t)$ vs t for an $n = 216$ homopolymeric melt on a cubic lattice[24] with $\phi = 0.5$, $n_B = 18$, and $r_{\rm min} = 5$. The curve is well fit by a sum of three exponentials. The majority (64%) of the contacts decay within 1% of τ_R, 91% of the contacts have decayed within 9% of τ_R, and the remaining 9% of the contacts decay on the order of τ_R. Thus, while the decomposition of the $n_c(t)$ vs t curve is by no means unique, long-lived dynamic contacts, i.e., dynamic entanglements, are rare events. The mean numbers of monomers (i.e., beads) between dynamic entanglements n_d is about 133. This is an order of magnitude larger than the static excluded volume screening length.

We next examined[24] the motion of the dynamic entanglements. Plots of $g_{\rm lab}(t)$ and $g_{\rm rel}(t)$ vs time are presented in Fig. 2. For all times studied up to τ_R, we found that $g_{\rm rel}(t)$ is just slightly less than twice $g_{\rm lab}(t)$. The difference in the ratio of $g_{\rm rel}(t)/g_{\rm lab}(t)$ from two probably arises from the fact that the rare, long-lived entanglements move slower.

We are now in a position to examine the differing physical effects of these two types of entanglements on the diffusive motion of the chains. These effects will then be built into the many-body treatment of diffusion presented in the next section. We use a standard separation of time scales argument. Those events which happen on a time scale fast compared to the time scale of interest can be treated in a mean field fashion. Thus the majority of the contacts which are short lived when compared to the terminal relaxation time can be averaged over. These contacts behave like scattering events between a chain and a solvent (in this case the other chains) but due to their short-lived nature have no topological effect on the chain. Hence the effect of these short-lived contacts can be subsumed into a phenomenological, molecular weight independent monomer (i.e., bead) friction constant. Thus, a melt of short chains experiences only the frictional effect of the short-lived contacts and behaves like a collection of Rouse chains, in agreement with experiment.[1] For a concentrated solution of chains, the frictional contribution of the short-lived chain–chain collisions and of the solvent collisions are lumped together into a single, phenomenological monomer friction constant.

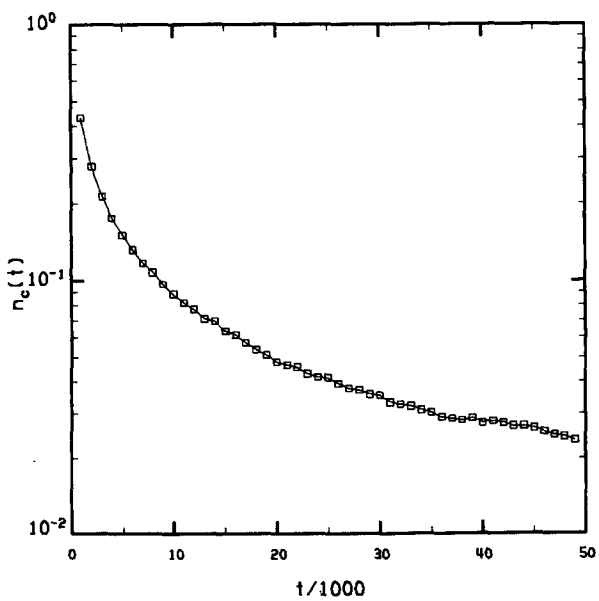

FIG. 1. Log–log plot of the number of dynamic contacts that survive up to a time t, $n_c(t)$ vs t for a $n = 216$ homopolymeric cubic lattice melt with $\phi = 0.5$, $n_B = 18$, and $r_{\rm min} = 5$. See the text for further details.

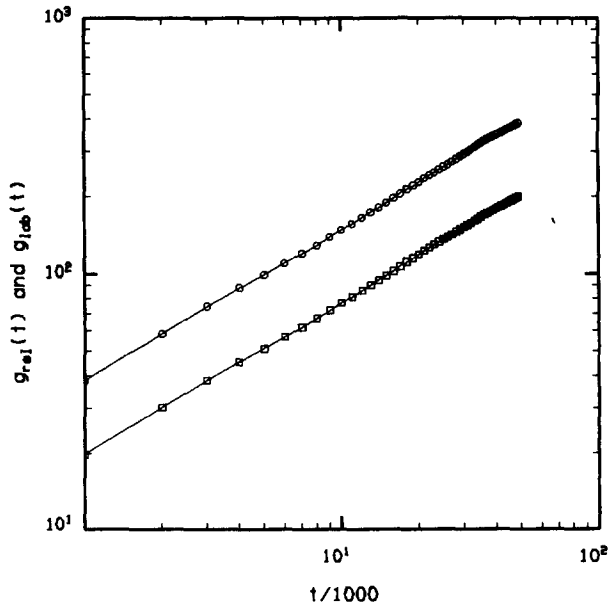

FIG. 2. The upper curve denoted by the circles is a log–log plot of the relative mean-square displacement of a pair of blobs belonging to different chains that are in contact at $t = 0$, $g_{\rm rel}(t)$, vs time. The lower curve denoted by the squares is a log–log plot of $g_{\rm lab}(t)$, the relative displacement of the center-of-mass of the pair of blobs with respect to the laboratory vs time, $n = 216$, $\phi = 0.5$, $n_B = 18$, and $r_{\rm min} = 5$.

The long-lived dynamic entanglements, being on the same time scale as the phenomena of interest, must be handled explicitly. However, here we are helped by the fact that dynamic entanglements are rare events—or said another way, the mean distance between dynamic entanglements (n_d) is large. Thus, even though we are dealing with a very dense system, by using the time scale separation to include the effect of the majority of contacts (the short-lived ones) in the monomer friction constant, we can treat the system as a dilute solution of dynamic contacts. Since we are really in a (renormalized) dilute solution limit we can safely truncate the many-body treatment at the pair contribution level. This is not to say that the effect of dynamic entanglements is small in the perturbation sense, since it certainly is not, but rather that true three-body interactions are so rare as to be completely negligible. Furthermore, between the dynamic entanglements, the chain can be treated as a dilute solution Rouse chain with a renormalized friction constant.

Thus, although our many-body treatment of chain diffusion to be presented in the next section will look formally identical to Hess' treatment[13] it will be physically quite different. Hess treated all interchain contacts explicitly in order that the contacts should constrain the chains to reptate.

Having been forced by our computer simulations to abandon the reptation model, we are only treating a very small number of the contacts, the long-lived ones, explicitly. Thus, Hess, when he truncates at the pair level, can only really treat physically dilute systems, while we can handle physically dense systems using the same truncation.

III. MANY-BODY TREATMENT OF DIFFUSION

As discussed above, our treatment of diffusion in polymer melts closely follows Hess' analysis.[13] Therefore we will not go through a full derivation of the equations. Rather we shall point out the physical assumptions in Hess' derivation and where, towards the end of the derivation, our assumptions differ from his. The reader who wants to see the mathematical steps should refer to Hess' paper (a copy of which he/she might wish to keep handy).

Starting from a Kubo expression for the diffusion constant in terms of the center-of-mass velocity autocorrelation function,

$$D=\frac{1}{3}\int_0^\infty dt\,\langle \mathbf{v}(t)\cdot\mathbf{v}(0)\rangle \tag{3.1}$$

(or equivalently, defining the diffusion constant using the long time limit of the mean-square displacement of the center-of-mass) Hess obtains using a Mori-type projection operator technique,

$$D=k_BT/n\left[\zeta_0+\int_0^\infty dt\,\Delta\zeta(t)\right]. \tag{3.2}$$

Here ζ_0 is a generalized, concentration dependent Rouse–Zimm monomer friction coefficient and $\Delta\zeta$ is a dynamic friction term per monomer due to the interaction between different polymer chains. In our approach, the effects of the short-lived contacts are to be included in ζ_0, leaving only the dynamic entanglement effects to be treated in $\Delta\zeta$. The dynamic friction function is given by

$$\Delta\zeta(t)=\frac{1}{3nk_BT}\langle \mathbf{F}(t)\cdot\mathbf{F}(0)\rangle, \tag{3.3}$$

where the correlation function is a Mori projected force autocorrelation function.

In order to obtain a tractable expression for the dynamic friction constant, Hess assumes that only short-ranged interactions occur between the polymer chains thus completely screening out the hydrodynamic interactions[25] (this assumption holds for melts) and further characterizes the interactions as steric in nature (excluded volume interactions). He then identifies the dynamic evolution of the friction constant with the dynamic evolution of the contacts between chains. He assumes a small number of contacts; hence he restricts himself to the semidilute regime. This leads to the treatment of the global motion of the chains as uncorrelated and to the truncation of the interactions at the pair level, i.e., no consideration of correlated three-body interactions is made. Since, as discussed in the previous section, we are treating only the long-lived contacts (which have a lifetime on the order of the terminal relaxation time) explicitly, we can also make use of Hess' semidilute approximation despite the fact that we are treating a dense system.

Hess then explicitly introduces the propagator of the dynamic friction term that describes the time evolution of pairs of contacts between chains, $R(t)$ (which he also refers to as the response function). Since one is interested only in the diffusional behavior of the polymers, one need only consider the long wavelength limit of the propagator [recall that the short wavelength behavior, i.e., the short time and distance contacts between chains, is subsumed into the effective renormalized Rouse–Zimm friction constant of Eq. (3.2)]. In this long wavelength limit, the propagator is dominated by the hydrodynamic pole and is given by

$$R(q,t)=\exp(-D_{\text{eff}}q^2t), \tag{3.4}$$

where q is the magnitude of the wave vector and D_{eff} is an effective diffusion constant.

It is in the identification of D_{eff} that we finally part company with Hess' treatment of diffusion. He has assumed that the forces are transverse to the chain axis and then arrives at reptation-like diffusion. He decomposes the motion into components parallel and perpendicular to the chain axis. Since the propagator is for long, but not very long, times (see below), Hess recognizes that he cannot just replace D_{eff} by $D_\parallel$ which would then be identified with the self-diffusion constant, but that he must weakly couple the perpendicular and parallel modes. He does this by factoring the propagator into the product of a parallel and a perpendicular propagator which is equivalent to setting $D_{\text{eff}}=D_\perp+D_\parallel$. If he did not do this, he would obtain the solution that the diffusion constant was identically zero for large, but finite n.

From our simulation results, we know that we need a propagator for times on the order of the terminal relaxation time. For such times we have observed in our simulations that the behavior of the chains is essentially Rouse like (see, e.g., Fig. 15 of Ref. 16 and the discussion therein). However there is also coupling between the center-of-mass coordinate and the internal (Rouse-like) coordinates. We can accommodate this physics by setting

$$D_{\text{eff}}=(1-\beta)D_0+\beta D, \tag{3.5}$$

where D_0 is the renormalized Rouse diffusion constant and β, which is small, gives the coupling between the center-of-mass motion and the internal coordinates.

Using Eqs. (3.5) and (3.4) in Hess' formulation we obtain

$$D=\frac{D_0}{1+\psi(c,n)D_0/[(1-\beta)D_0+\beta D]}, \tag{3.6}$$

where $\psi(c,n)$ is related to the free energy change per chain per dynamic entanglement which in turn must be proportional to the number of dynamic entanglements per chain. Thus, the mean number of monomers between entanglements, n_e, is defined by

$$\psi=n/n_e. \tag{3.7}$$

As shown in the Appendix, n_e is inversely proportional to c; with c being the concentration of polymer segments/unit volume. Using the expression for the Rouse diffusion constant

$$D_0 = \frac{kT}{n\zeta_0} = \frac{d_0}{n}, \tag{3.8}$$

where ζ_0 is the renormalized monomer friction constant and Eq. (3.7) in Eq. (3.6),

$$D = D_0(2(1-\beta)/\{1 - 2\beta + n/n_e + [1 + 2(1-2\beta)n/n_e + n^2/n_e^2]^{1/2}\}). \tag{3.9}$$

In the limit that $\beta \to 0$, it follows from Eq. (3.9) that

$$D = \frac{D_0}{1 + n/n_e} \tag{3.10a}$$

$$= \frac{d_0}{n + n^2/n_e}. \tag{3.10b}$$

It is also apparent from Eq. (3.9) that for all $\beta \neq 1$, in the limit of large n/n_e,

$$D = D_0(1-\beta)n_e/n = d_0(1-\beta)n_e/n^2. \tag{3.11}$$

Moreover, for all β if $n/n_e = 0$, we have

$$D = D_0, \tag{3.12}$$

that is, the free Rouse value of D is recovered.

The above behavior is confirmed in Fig. 3 where we plot D/D_0 vs n/n_e calculated from Eq. (3.9) for $\beta = 0.0$, 0.5, and 0.9 in the curves going from top to bottom. In all cases the large n/n_e regime is consistent with n^{-2} behavior. The crossover region from constant behavior to the $D/D_0 = (1-\beta)n_e/n$ limit is fairly smooth, but the magnitude of the slope increases with increasing β. In fact, for $\beta = 0.9$, the slope of the $1 \leqslant D/D_0 \leqslant 3$ crossover regime is -1.52. This apparently increased slope as a function of n is in fact a remnant of the glass transition that occurs at $n/n_e = 1$ when $\beta = 1$.

Rewriting Eq. (3.9) by multiplying the numerator and denominator by $-(1-2\beta + n/n_e) + [1 + 2(1-\beta)n/n_e + n^2/n_e^2]^{1/2}$ gives

$$D = D_0\{-[(1-2\beta) + n/n_e] + [1 + 2(1-2\beta)n/n_e + n^2/n_e^2]^{1/2}\}/2\beta. \tag{3.13}$$

In the limit that $\beta \to 1$ Eq. (3.13) becomes

$$D = D_0(1 - n/n_e) \quad \text{if } n \leqslant n_e \tag{3.14a}$$

$$= 0 \quad \text{if } n \geqslant n_e. \tag{3.14b}$$

Thus, Eq. (3.14) predicts a glass transition, i.e., $D = 0$ when $\beta = 1$ and $n \geqslant n_e$. The origin of the glass transition is as follows: Setting $\beta = 1$ is equivalent to using $D_{\text{eff}} = D$ in the expression for the propagator in Eq. (3.4). We interpret this as the limit where even for the short-time propagator the system is so tightly coupled that the motion requires the full diffusion constant rather than a "free" Rouse diffusion constant or free Rouse propagator. When the system is this tightly coupled, and each chain pulls another chain, which pulls another chain, etc., the physical model has broken down and the $D = 0$ solution signifies that the tightly coupled system is not a melt at all but a glass. Equations (3.14a) and (3.14b), when plotted on a log–log plot, would give a line whose slope is infinite in magnitude. This is the origin of the increased slope in the curve having $\beta = 0.9$ in Fig. 3 when n/n_e is on the order of unity.

Equation (3.14b) implies that the glass transition temperature should be molecular weight independent for sufficiently long polymers. Furthermore, if we assume that $\beta = \beta(c,T)$, then polymers which are substantially below the entanglement molecular weight should not undergo a glass transition due to the effect of entanglement trapping. This is consistent for example with experimental measurements on the viscoelastic behavior of polystyrene (PS) whose entanglement molecular weight is about 18 000.[26] PS of nominal molecular weight 4000 has a glass transition temperature $T_g^\circ = 64$ °C, which is substantially below the glass transition temperature of high molecular polystyrene whose T_g is 100 °C.[27] This is qualitatively interpreted as follows: high molecular weight samples with $n > n_e$, undergo a glass transition temperature because of the shut down of a global mode—the disengagement of dynamic entanglements. Thus, T_g for high molecular weight samples is molecular weight independent. Low molecular weight polymer liquids are conjectured to undergo a glass transition because of the shut down of local configurational changing fluctuations, such as was seen in our diamond lattice Monte Carlo simulations.[15]

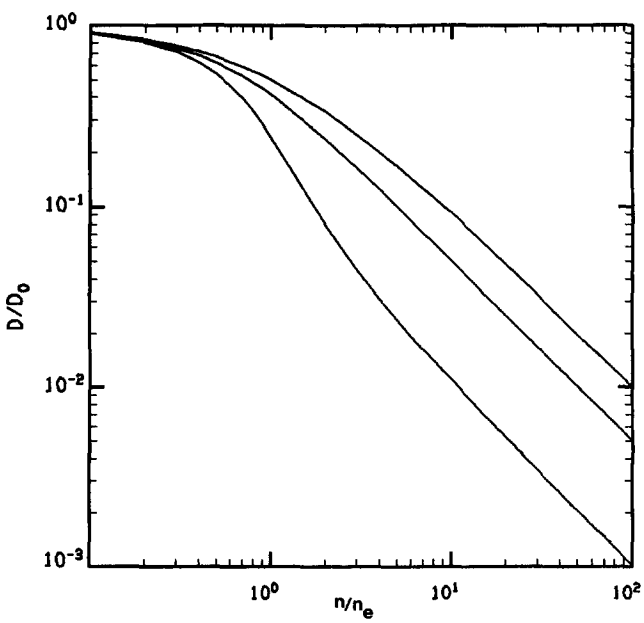

FIG. 3. Log–log plot of D/D_0 vs n/n_e calculated from Eq. (3.9) for $\beta = 0$, 0.5, and 0.9 in the curves going from top to bottom.

A. Polymer probe diffusion in a polymer matrix of different molecular weight

We shall now briefly discuss how one can modify the diffusion theory given above to accommodate the case when a probe polymer of degree of polymerization n_p is diffusing in a melt of polymers with a degree of polymerization n_m. It is assumed throughout that the concentration of probe polymers is small enough that a probe polymer only interacts with matrix polymers—it never encounters another probe polymer. Generalization to a finite volume fraction is straightforward.

The theory goes through exactly the same as before ex-

cept that the dynamic friction term $\Delta\zeta$ describes the dynamic evolution of a contact between a probe polymer and a matrix polymer. Hence the propagator $R(t)$ is that appropriate to the time evolution of a dynamic entanglement between a probe polymer and a matrix polymer. Thus, when we take the long wavelength (hydrodynamic) limit of the propagator in Eq. (3.4), we must use an effective diffusion constant for the probe-matrix pair. Consistent with the discussion of the physics contained in D_{eff} in the preceding subsection, we can accomplish this by setting

$$D_{\text{eff}} = (1-\beta)\left[\gamma D_{0p} + (1-\gamma)D_{0m}\right] + \beta\left[\gamma' D_p + (1-\gamma')D_m\right]. \tag{3.15}$$

Here $p(m)$ refers to a probe (matrix) polymer chain and again D_0 is the renormalized Rouse diffusion constant and D is the center-of-mass diffusion constant. Of course in the long time asymptotic region, a mutual diffusion constant is just the average of the diffusion constants. However, we do not really know how to take the averages in the intermediate time regime when the propagator is of interest; hence we leave γ and γ' as adjustable constants to be fit by experiment. Obviously when the probe and matrix polymer chains are identical, Eq. (3.15) reduces to the previous result, Eq. (3.5)

Using Eq. (3.15) in the Hess formalism, we obtain for the diffusion constant of the probe polymer

$$D_p = \frac{d_0}{n_p}\left[\frac{-(B-\beta\gamma'+n_p/n_e)+\{(B-\beta\gamma'+n_p/n_e)^2+4\beta\gamma' B\}^{1/2}}{2\beta\gamma'}\right], \tag{3.16a}$$

wherein

$$B = (1-\beta)\left[\gamma+(1-\gamma)n_p/n_m\right] + \beta(1-\gamma')\frac{D_m}{D_{0m}}n_p/n_m, \tag{3.16b}$$

and D_m is given by Eq. (3.9) on setting $n = n_m$. D_{0m} is the self-diffusion coefficient the matrix would have in the absence of entanglements.

Several limiting cases of the above functional form are readily obtained. Consider first the limit that $n_p/n_e = 0$ (that is, the probe chain is so short that there are no dynamic entanglements). It immediately follows from Eq. (3.16a) that

$$D_p = \frac{d_0}{n_p}; \quad n_e/n_p \ll 1. \tag{3.17}$$

That is, the unentangled Rouse limit of the self-diffusion coefficient is recovered. Physically, this makes sense. If the probe chain is sufficiently short that there are no dynamic entanglements, it should diffuse through uninterrupted by such constraints.

Another physically interesting limit of Eq. (3.16a) is obtained if $\beta \neq 1$ and $n_p/n_e \gg 1$ and $n_p/n_m < 1$, that is, an entangled probe chain in a matrix of long entangled chains. After a bit of arithmetic, Eqs. (3.16a) and (3.16b) give

$$D_p = \frac{d_0}{n_p}\left[(1-\beta)\gamma\frac{n_e}{n_p} + (1-\beta)(1-\gamma)\frac{n_e}{n_m}\right]. \tag{3.18a}$$

Observe that when $n_p = n_m$, Eq. (3.11) is recovered. That is, $D_p \sim n_p^{-2}$. In the limit that n_m goes to infinity,

$$D_p = (1-\beta)\gamma\frac{n_e}{n_p^2}d_0. \tag{3.18b}$$

That is, D_p is reduced from the $n_m = n_p$ result by a factor of γ.

Equation (3.18a) predicts a much weaker matrix molecular weight dependence, $D_p \sim n_m^{-1}$, than the constraint release models invoked to make reptation theory self-consistent. Graessley[4(b)] has derived an expression for the contribution of self-diffusion due to reptation of the entanglements that form the tube which is of the form

$$D_{\text{cr}} \sim n_e^2/(n_p n_m^3). \tag{3.19a}$$

Klein[11(b)] has argued that not all the constraints relax independently, and in the nonindependent constraint release (nicr) model

$$D_{\text{nicr}} \sim n_e^{3/2}/(n_p n_m^{5/2}). \tag{3.19b}$$

Thus, the diffusion constant of a reptating chain including constraint release is of the form

$$D = \frac{d_0}{3}n_e/n^2 + D_{\text{tube}} \tag{3.20}$$

with D_{tube} given by Eqs. (3.19a) or (3.19b).

The most extensive experimental test of the above functional forms Eqs. (3.19) and (3.20) has been done by Green and Kramer[28] on the probe diffusion coefficient in bidisperse polystyrene melts. The probes spanned the range of molecular weight from 55 000–2 000 000 and the matrices ranged in molecular weight from 2100 to 20 000 000. Antonietti, Coutandin, and Sillescu[20] have also performed a series of diffusion constant measurements over a less extensive molecular weight range, which is in agreement with the Green and Kramer results where the two sets of measurements overlap. Green and Kramer find a matrix molecular weight dependence consistent with both Graessley and Klein [Eq. (3.19a) and Eq. (3.19b)], although they prefer the former expression. However, McKenna[29] has pointed out that the use of either Eqs. (3.19a) or (3.19b) is inconsistent with the experimentally observed D when $n_m = n_p$, i.e., $D \sim n^{-2}$. Thus, the experimental situation is not entirely clear. On the other hand, we point out that Eq. (3.18a) reduces to the $n_m = n_p$ result and gives $D \sim n^{-2}$.

In Fig. 4, we plot D_p/D_{0p} calculated via Eqs. (3.16a) and (3.16b) vs n_m/n_e for $n_p/n_e = 1$, 5, 10, and 50 in the curves going from top to bottom. In all cases $\beta = 0$; thus D_p explicitly equals

$$D_p = \frac{d_0}{n_p}\left[\frac{\gamma+(1-\gamma)n_p/n_m}{\gamma+(1-\gamma)n_p/n_m+n_p/n_e}\right]. \tag{3.21}$$

Increasing n_p is seen to increase the breadth of the transition to n_p^{-2} behavior—otherwise stated, a larger absolute value

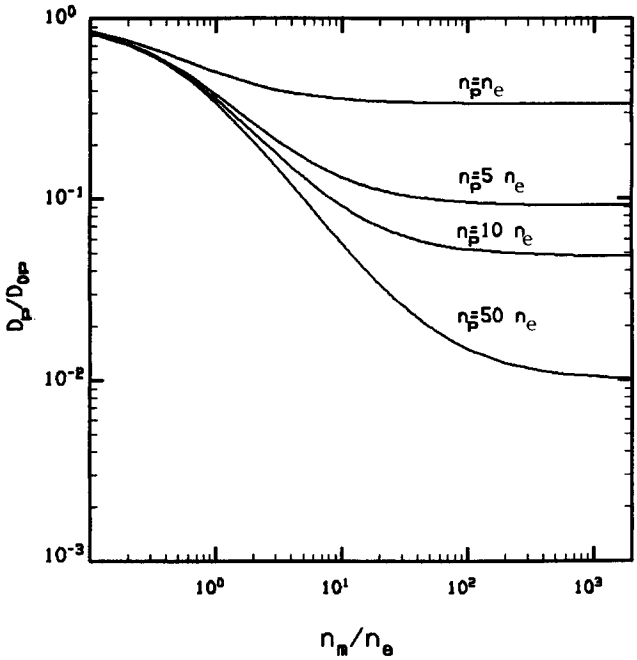

FIG. 4. Log–log plot of D_p/D_{0p} calculated via Eq. (3.16) vs n_m/n_e for $n_p/n_e = 1$, 5, 10, and 50 in the curves going from top to bottom. $\beta = 0$, $\gamma = 0.5$.

n_m is required before the $n_m \to \infty$ limit is reached. Observe, too, that in the limit that n_m goes to zero, all the curves coalesce to the same value of D_p/D_{0p}; we consider this point next.

It immediately follows from Eq. (3.21) that in the limit $n_p/n_m \gg 1$ and $n_m \ll n_e$, that $D_p = D_{0p}$; i.e., the chain is no longer in an entangled environment, and thus the free Rouse result with a molecular weight independent friction constant appropriate to the matrix must be recovered. Thus all the curves shown in Fig. 4 coalesce to the value unity in the limit $n_m/n_e \ll 1$.

Consider next the case when $n_m \gg n_e$, $n_p \gg n_e$, and $n_p > n_m$. That is, the case of a very long polymer in an entangled matrix. Provided that $\beta \neq 1$, it follows from Eq. (3.16a) and (3.16b) that

$$D_p = D_{0p}\left[\frac{1}{1+(n_m/n_e)1/\{(1-\gamma)(1-\beta)\}}\right] \quad (3.22a)$$

$$\simeq d_0 \frac{(1-\gamma)(1-\beta)n_e}{n_p n_m}. \quad (3.22b)$$

Thus, the apparent monomeric friction constant is augmented by a factor $n_m/[n_e(1-\gamma)(1-\beta)]$. The probe self-diffusion coefficient increment D_p/D_p^0 is now independent of n_p, and behaves as if it were in a medium of friction constant $\zeta_0 n_m/[n_e(1-\gamma)(1-\beta)]$. Observe however, that the Stokes–Einstein limit is not reached since $\eta_m \sim n_m^{3.4}$. Rather Eq. (3.22a) predicts that the viscosity relevant to the diffusing chain is the Rouse value $\eta_{0m} \sim n_m$. However, caution must be employed here. Remember ζ_0 itself contains the high frequency contribution of the matrix collisions with the probe. So in fact Eqs. (3.22a) and (3.22b) are valid only over an intermediate regime of molecular weights, and provide an $\zeta_0 \sim n_m$. As $n_p \gg n_m$, ζ_0 should be replaced by the Stokes–Einstein value $6\pi\eta_m a$ with a being the effective radius of a monomeric bead. Moreover, neglect of hydrodynamic interactions will no longer be valid. Including both these effects in the limit that $n_p \gg n_m > n_e$ we should have

$$D_p \sim n_m^{-3} n_p^{-1/2}, \quad (3.23a)$$

thereby recovering a result previously derived by de Gennes in his classic book.[3]

In Figs. 5A–5C, we present a log–log plot of D_p/D_{0p} vs n_m/n_e calculated via Eqs. (3.16a) and (3.16b) for chains having $n_p/n_e = 1$, 10, and 50, respectively. In each figure, $\beta = 0$, 0.5, and 0.9 in the curves going from top to bottom, respectively, and $\gamma = \gamma' = 0.5$. As required, all the curves coalesce to unity as $n_m/n_e \to 0$. Furthermore, the apparent slope in the vicinity of $n_m/n_e = 1$ increases as $\beta \to 1$. More explicitly, in the limit that $\beta \to 1$, Eqs. (3.16a) and (3.16b) require the following. [Remember that when $n_m = n_e$, the self-diffusion coefficient of the matrix, D_m, goes to zero, see Eqs. (3.14a) and (3.14b).] If $n_m < n_e$, we have

$$D_p = D_{0p}/2\gamma'\left\{-\left[(1-\gamma')\left(\frac{n_p}{n_m}-\frac{n_p}{n_e}\right)-\gamma'+n_p/n_e\right]\right.$$
$$+\left[\left[(1-\gamma')\left(\frac{n_p}{n_m}-\frac{n_p}{n_e}\right)-\gamma'+\frac{n_p}{n_e}\right]^2\right.$$
$$\left.\left.+4\gamma'(1-\gamma')\left(\frac{n_p}{n_m}-\frac{n_p}{n_e}\right)\right]^{1/2}\right\}, \quad (3.23b)$$

where we have used Eq. (3.14a) for D_m. Thus, if $D_m \neq 0$ ($n_m < n_e$), then $D_p \neq 0$ independent of n_p. However, if $D_m = 0$ ($n_m \geqslant n_e$), then

$$D_p = D_{0p}^0(1 - n_p/\gamma' n_e) \quad \text{if } n_p/n_e < \gamma', \quad (3.24a)$$

$$= 0 \quad \text{if } n_p/n_e \geqslant \gamma'. \quad (3.24b)$$

Thus, the following behavior for D_p is predicted for diffusion of a probe in a glass: If $n_p/\gamma' n_e < 1$, then the effects of dynamic entanglements are insufficient to produce a glass transition for the probe. However, if n_p/n_e exceeds γ' (a number between zero and unity), then the probe is predicted to have a zero self-diffusion coefficient. Thus, in agreement with real experiments, relatively small molecular weight probes can readily diffuse through an entangled polymer glass, yet larger molecular weight species are predicted to have $D_p = 0$. The glass transition for the probe occurs at lower values of n_p than for the matrix, since the effective propagator between the dynamic entanglements $D_{\text{eff}} \sim \gamma D_p$, when $\beta = 1$ and $D_m = 0$.

B. Comparison with simulations

We have fit Eq. (3.10b) for the self-diffusion constant to our cubic lattice simulation for a homopolymeric melt.[17] The fit to the data (three data points with $n = 64$, 100, and 216) was very good with the average error being 1.4%. This was well within the average statistical error of the simulation which is 1.8%. We obtained best fit values of $d_0 = 0.16$ and $n_e = 125$. Recall that the dynamic entanglement length we obtained by counting the long-lived contacts was 133. When the value of the diffusion constant for $n = 800$ was calculat-

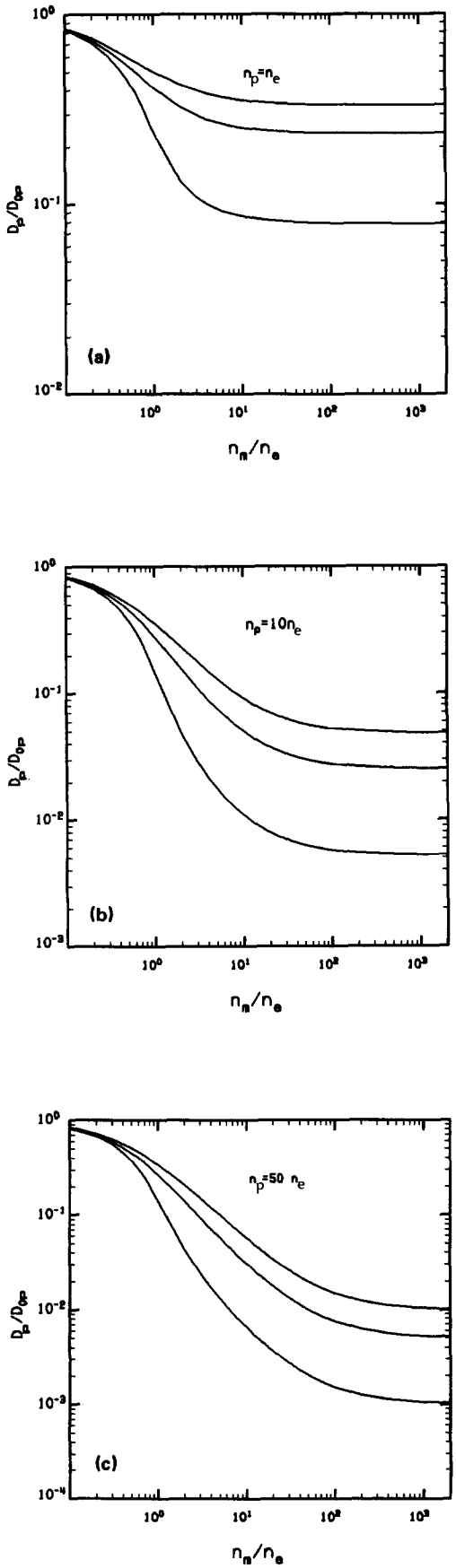

FIG. 5. A–C. Log–log plot of D_p/D_{0p} vs n_m/n_e calculated via Eqs. (3.16a) and (3.16b) for a probe chain having $n_p/n_e = 1$, 10, and 50, respectively. In each figure, curves going from top to bottom are, $\beta = 0$, 0.5, and 0.9 and $\gamma = \gamma' = 0.5$.

ed using these parameters (the $n = 800$ system was not in the data set used to obtain the parameters) we obtained $D = 2.71 \times 10^{-5}$. This is in good agreement with the extrapolated upper bound for the diffusion constant of 2.8×10^{-5} (the lower bound is 1.2×10^{-5}). This suggests that the extrapolated upper bound is closer to the correct simulation diffusion constant for $n = 800$ than is the lower bound.

For the case of a probe polymer diffusing in a matrix with a different degree of polymerization[18] ($n_p = 100$; $n_m = 50$, 100, 216, and 800), we used Eq. (3.21). If we just used the parameters from the homopolymeric fit, and the asymptotic form for D_{eff}—the average of the two diffusion constants, i.e., $\gamma = 0.5$—we obtain a fit to the simulation with an average error of 7.2%. This compares well to the statistical error of the simulation of 4.6%. If we treat the mixing parameter γ as being adjustable and still use the homopolymeric results for d_0 and n_e, we obtain a $\gamma = 0.677$ and an average error in D_p of 5.0%, essentially the statistical error. In order to test the sensitivity, we also fit the simulations using the homopolymeric result for $d_0 = 0.16$, the asymptotic mixing coefficient of $\gamma = 0.5$ and let the entanglement distance n_e be a free parameter. This results in a quite respectable fit with an average error of 6.4% and a value for n_e of 129. Thus we obtain a value for the entanglement distance that is, for all practical purposes, the same as that for the homopolymeric melt. It is also clear, insofar as we can judge from the present data, that the theory is not overly sensitive to the mixing parameter γ, and it appears that one can safely use the asymptotic value of 1/2.

IV. CONCLUSIONS

In this paper we have shown, using an adaptation of Hess' general many-body theory of polymer diffusion in dense systems, that one can obtain the experimental scaling behavior with molecular weight of the diffusion constant of a polymer melt [Eq. (1.1)], using only a few very general physical assumptions. The necessary physical assumptions are:

(i) The long distance global motions of the various chains are uncorrelated.

(ii) The important chain–chain interactions which lead to the $D \sim n^{-2}$ behavior in the entangled regimes are the long-lived entanglements; i.e., those interchain contacts whose lifetimes are of the order of a terminal relaxation time. From our computer simulations we have observed that only a small number of chain–chain contacts lead to such long-lived dynamic entanglements, $\sim 10\%$. Hence, the distance between dynamic entanglements is large, $n_d \simeq 130$, and the dense polymer system can be treated as a dilute system of dynamic entanglements. This leads to a sensible truncation of the many-body treatment at the pair level with the effects of short time contacts being subsumed into the single body renormalized monomer friction constant.

(iii) The propagator for the time development of dynamic contacts is essentially a free renormalized Rouse propagator. Hence, the theory essentially takes the form of a lowest order perturbation expansion about a renormalized Rouse theory. This is consistent with our simulations which showed that the behavior of the chains is largely Rouse-like.

The natural simple physical picture which emerges from this work as well as our simulations is that the scaling behavior $D \sim n^{-2}$ for the diffusion of entangled chains is caused by long time dynamic contacts between pairs of chains as one chain pulls another through the melt. We can picture a dynamic entanglement (perhaps somewhat over simplistically) as a loop formed by one chain about the other, that results in one chain randomly dragging the other. Of course, in time the random motion of the chains causes the pair to separate. From our simulation results, dynamic contacts are destroyed mainly from the chains just randomly diffusing apart, i.e., the chains move in different directions, rather than by the slithering of chains past each other as in the reptation model. However, on average, the chains having broken one dynamic entanglement are also forming other dynamic entanglements at the same time (albeit in different places on the chain). Thus, one can picture a chain's diffusive progress through the melt as a continuing overlapping series of forming dynamic entanglements, dragging another chain for a while, and then breaking off the entanglement by moving apart. The entanglement distance of $n_e = 125$ we obtained by fitting the self-diffusion constant [Eq. (3.9)] to our simulation results [or $n_e = 129$ by fitting Eq. (3.16)] should be looked upon as a statistically averaged distance between entanglements, and thus is not directly comparable with n_d (the mean distance between entanglements that live on the order of the terminal relaxation time). However, it is still gratifying that the two numbers should be so close (well within the errors). This is at least evidence (permissive but by no means compulsive) for the internal consistency of the picture.

Lastly, we turn to the fact that $D \sim n^{-2}$ has frequently been claimed as experimental evidence for the essential correctness of the reptation model of polymer motion. Clearly from the very general nature of the physical assumptions which were necessary to derive the scaling behavior of the diffusion constant, there are a very large class of physical models of polymer motion which will reproduce this scaling behavior. We shall in fact present a member of this class in our companion paper which treats the viscoelastic behavior of polymer melts. Of course, this model is consistent with the picture given above. At best the experimental diffusion scaling behavior can be used as permissive evidence for a model (in that it is not immediately discarded) but cannot in any way be used to say that the essential correctness of any model of polymer motion is experimentally confirmed. Rather, a $D \sim n^{-2}$ is merely indicative that some kind of constrained motion of the polymer has become operative.

ACKNOWLEDGMENTS

This research was supported in part by Grant No. DMR-25-20789 of the Polymer Program of the National Science Foundation and in part by Grant No. GM-37408 from the Division of General Medical Sciences, United States Public Health Service. We wish to thank Dr. W. Graessley for useful comments and a stimulating discussion and the referee for timely criticism and suggestions, and the careful reading of the manuscript.

APPENDIX: DERIVATION OF THE CONCENTRATION DEPENDENCE OF n_d

$\psi(c,n)$ of Eq. (3.6) is given by

$$\psi = \tfrac{2}{3} n \Delta F / c k_B T, \tag{A1}$$

where $c = nN/V$ with N the number of polymer molecules in the system of volume V. As shown by Hess in the single contact approximation,[13] the free energy density which arises from interactions between pairs of chains, ΔF, is

$$\Delta F = k_B T v_0 / 2 V N^2 n^2 \langle \delta(R_{ij}) \rangle, \tag{A2}$$

with R_{ij} the distance between a segment i on chain 1 and a segment j on chain 2. In writing Eq. (A2) we are explicitly neglecting end effects. v_0 is the effective volume excluded between a pair of segments which in the dilute limit is concentration independent. The brackets denote the ensemble average. Remembering that with respect to the dynamic contacts we are in the dilute solution limit, we have

$$\langle \delta(R_{ij}) \rangle = 1/V \int dR_{12}\, \delta(R_{12}) \tag{A3a}$$

$$= V^{-1}. \tag{A3b}$$

In writing Eq. (A3), we truncate at the level of two body terms. Observe that $k_B T v_0 / V$ is the ensemble average of a Mayer f function. Thus, we have

$$\Delta F = k_B T c^2 v_0 / 2. \tag{A4}$$

Substituting Eq. (A4) into Eq. (A1) gives

$$\psi = c v_0 n / 3$$

and defining n_e by

$$\psi = n / n_e$$

gives

$$n_e = 3 / v_0 c.$$

Thus, in agreement with measurements of the plateau modulus,[4] n_e is inversely proportional to the concentration of polymer segments/unit volume.

[1] J. D. Ferry, *Viscoelastic Properties of Polymers* (Wiley, New York, 1980).
[2] P. G. de Gennes, J. Chem. Phys. **55**, 572 (1971).
[3] P. G. de Gennes, *Scaling Concepts in Polymer Physics* (Cornell University, Ithaca, 1979).
[4] (a) W. W. Graessley, Adv. Polym. Sci. **16**, 1 (1974); (b) **47**, 67 (1982).
[5] H. Kim, T. Chang, J.M. Yohanan, L. Wang, and H. Yu, Macromolecules **19**, 2737 (1986).
[6] G. D. J. Phillies, Macromolecules **19**, 2367 (1986).
[7] S. F. Edwards, Proc. Phys. Soc. **92**, 9 (1967).
[8] P. G. de Gennes, Macromolecules **9**, 587, 594 (1976).
[9] M. Doi and S. F. Edwards, J. Chem. Soc. Faraday Trans. 2 **74**, 1789, 1802, 1818 (1978); **75**, 38 (1978).
[10] R. B. Bird, C. F. Curtiss, R. C. Armstrong, and O. Hassager, in *Dynamics of Polymeric Liquids, Vol. 2. Kinetic Theory*, 2nd ed. (Wiley, New York, 1987).
[11] (a) J. Klein, Macromolecules **11**, 852 (1978); (b) **19**, 105 (1986).
[12] M. Daoud and P. G. de Gennes, J. Polym. Sci. Polym. Phys. Ed. **17**, 1971 (1979).
[13] W. Hess, Macromolecules **19**, 1395 (1986).
[14] See, e.g., A. Baumgartner, Annu. Rev. Phys. Chem. **35**, 419 (1984).
[15] A. Kolinski, J. Skolnick, and R. Yaris, J. Chem. Phys. **84**, 1922 (1986).

[16]A. Kolinski, J. Skolnick, and R. Yaris, J. Chem. Phys. **86**, 1567 (1987).
[17]A. Kolinski, J. Skolnick, and R. Yaris, J. Chem. Phys. **86**, 7164 (1987).
[18]A. Kolinski, J. Skolnick, and R. Yaris, J. Chem. Phys. **86**, 7174 (1987).
[19]J. Skolnick and R. Yaris, J. Chem. Phys. **88**, 1418 (1988).
[20]M. A. Antonietti, J. Coutandin, and H. Sillescu, Macromolecules **19**, 793 (1986).
[21]P. F. Green, P. J. Mills, C. J. Palmstrom, J. W. Mayer, and E. J. Kramer, Phys. Rev. Lett. **53**, 2145 (1984).
[22]P. E. Rouse, J. Chem. Phys. **21**, 1272 (1953).
[23]H. Yamakawa, *Modern Theory of Polymer Solutions* (Harper and Row, New York, 1969), Chap. 6.
[24]These results were obtained from the MC trajectories of Ref. 17.
[25]K. F. Freed and S. F. Edwards, J. Chem. Phys. **61**, 3626 (1974).
[26]J. Lamb, in *Molecular Basis of Transitions and Relaxations Midland Macromolecular Monographs*, edited by D. J. Meier (Gordon and Breach, New York, 1978), Vol. 4, p. 52.
[27]T. G. Fox and P. J. Flory, J. Appl. Phys. **21**, 581 (1950).
[28]P. F. Green and E. J. Kramer, Macromolecules **19**, 1108 (1986).
[29]G. B. McKenna, Poly. Comm. **26**, 324 (1985).